Progress In Electromagnetics Research C, Vol. 119, 191–200, 2022

A Dual-Band High-Gain Substrate Integrated Waveguide Slot Antenna for 5G Application

Umesh Singh* **and Rajesh Mishra**

Abstract—In this paper, the authors propose a small substrate integrated waveguide (SIW) slot antenna for future fifth generation (5G) communication systems. It works at 28 and 38 GHz. The proposed geometry consists of horizontal and vertical vias as well as a central circular ring. The cut slots in the etched center circular ring create a significant capacitive loading effect, lowering the lower resonating mode. Further, the introduced circular ring slot resonates on TE_{101} and TE_{102} modes at 28 and 38 GHz, respectively. The measured impedance bandwidths are 27.77–28.02 GHz and 37.99–38.10 GHz. Peak gains in the lower and upper bands are measured to be 6.96–7.15 dBi and 8.10–8.22 dBi, respectively. At 28 and 38 GHz, the observed half-power beam-widths (HPBWs) are 74.5° and 79.2°, respectively. Considering these performance results, such as single-layer dual-bands, high gain, small size, and good radiation efficiency, the designed SIW slot antenna is suitable for future millimeter-wave 5G applications.

1. INTRODUCTION

A move to millimeter-wave (mmWave) operating frequencies is necessary to meet the demanding conditions for next-generation wireless systems. Innovative applications, such as 5G mobile communication, demand extremely high data rates. Furthermore, multi GHz bandwidths have become essential, which is the fundamental impetus for moving to mmWave frequencies. The 28 GHz (27.5–29.5 GHz) and 38 GHz (37–38.6 GHz) mmWave bands are being extensively explored for next-generation (5G) wireless systems, with considerable performance gains over fourth-generation (4G) networks [1]. Multi-band antennas are one of the best solutions for 5G communication as a single radiating element can cover multiple frequency ranges of interest. Also, antenna arrays will be necessary because of the increased path loss at high operating frequencies (28/38 GHz band). There is a trend to design compact antennas to decrease the size of electronic devices and hence integrate them with 5G equipment. However, antenna shrinking techniques frequently have unfavorable consequences on the device's operation. The compactness of an antenna is an important aspect but not at the expense of its performance. Hence, a compact, low-cost 5G antenna topology with good efficiency, gain, and bandwidth capabilities is required [1, 2].

Because of its low loss and high isolation, equivalent to rectangular waveguides made of solid metal, substrate integrated waveguide (SIW) attracts much attention in the mmWave research field [3]. It is also compatible with the common printed circuit board (PCB) manufacturing. Furthermore, because of the electromagnetic fields' confinement inside the SIW structure, it also possesses outstanding shielding properties. This enables active electronics to be integrated with proximity. Quarter-mode SIW (QMSIW) cavities are created by bisecting a rectangular SIW cavity twice along the two virtual quasi-magnetic walls. This approach produces tiny cavities with good microwave performance while

Received 8 February 2022, Accepted 29 March 2022, Scheduled 5 April 2022
* Corresponding author: Umesh Singh (umeshsingh2002@gmail.com).
The authors are with the School of Information and Communication Technology Department, Gautam Buddha University, Greater Noida, Uttar Pradesh, India.

preserving the original SIW cavity's field distribution [4–6]. In [7–16], high gain, low-profile SIW antennas for dual-band application are presented by introducing different geometries and cavities in the structure. In literature, the proposed geometries are complex in design. Also, it is difficult to fabricate, and implementation is challenging.

The authors present a dual-band high gain SIW slot antenna for future 5th generation applications in this paper. The proposed geometry is a combination of vias and center circular slotted ring. The circular slotted ring is responsible for the lower and higher resonating bands. The designed parameters are optimized, and parametric analysis has been performed in CST-MWS simulation software [17]. The proposed geometry resonates at 28.13 and 37.97 GHz with acceptable impedance bandwidth. In comparison with a state-of-the-art, the designed dual-band SIW is single-layered with small size ($7.50 \times 27.06\,\text{mm}^2$). The measured directivities at 27.90 and 38.05 GHz are 8.01 and 8.36 dBi. Also, they have a simulated radiation efficiency of 88.25% and 86.30%, respectively. The simulated and measured results are acceptable for the future 5G communication systems.

The rest of the paper is organized as follows. The proposed geometry step formation and parametric analysis are reported in Section 2. Section 3 presents the simulation and measurement findings. Finally, The suggested work's conclusion is presented in Section 4.

2. DESIGN PROCEDURE

The design method for a high gain dual-band slotted SIW antenna operating at 28 and 38 GHz is described in this part. The designed SIW slot antenna is depicted in top and bottom views in Figures 1(a) and (b). The suggested antenna is built on a Rogers RT-duroid 5880 substrate, which has a height of 0.254 mm, a dielectric constant ϵ_r of 2.2, and a loss tangent ($\tan\delta$) of 0.003. m_2 and m_1 are the antenna's total length and width. Metalized vias or holes are drilled through the antenna to create a SIW construction. Metalized vias and holes have a radius of 0.25 mm. The antenna construction includes two slots carved into the metallic plane of the SIW cavity to increase antenna performance. The slots are in the form of arcs of a circle with radius (D_1) 2.68 mm. The circle is cut with a length of 1.0 mm after an angle of θ_1 in the anticlockwise direction. Similarly, the second cut is made after an angle of $90^\circ + \theta_1$.

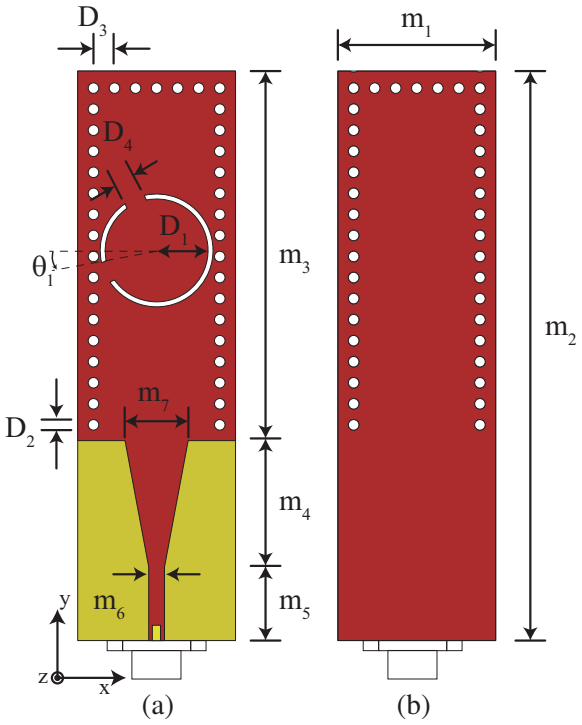

Figure 1. Schematic diagram of proposed SIW: (a) Top-view. (b) Bottom-view.

The designed antenna is excited with a 50 Ω proximity-feed microstrip line which has a width m_6 and length m_5. In order to connect microstrip line and designed SIW structure, a tapered geometry is incorporated. The width m_7 and length m_4 of the tapered shape are 3.0 and 6.0 mm, respectively, and it is used as the transition between microstrip and SIW structure. Also, it improves the impedance matching performance. The diameter of via D_2 is 0.5 mm, and the distance between two vias D_3 is 1.0 mm. Therefore, the designed geometry satisfies $D_3/D_2 < 2.5$. The detailed dimension of the designed SIW structure is given in Table 1.

Table 1. Detailed dimensions of the proposed SIW structure.

Symbol	m_1	m_2	m_3	m_4	m_5	m_6
Value (mm)	7.50	27.06	17.56	6.0	3.50	0.69
Symbol	m_7	D_1	D_2	D_3	D_4	θ_1
Value (mm)	3.0	2.68	0.5	1.0	1.0	10°

2.1. Step Formation of SIW

The step-by-step formation of the designed SIW slot antenna is as follows. In step 1, only horizontal vias are made, depicted in Figure 2(a). The corresponding S_{11} using this geometry can be seen in Figure 3 (Step 1). It can be seen that the antenna resonates at 34.5 GHz alone, which is in between our required frequencies. Next, in step 2, only vertical vias are made, as shown in Figure 2(b). The S_{11} of this geometry is not able to resonate at any frequency (shown in Figure 3 (Step 2)). Further, in step 3, horizontal and vertical vias are combined, as shown in Figure 2(c). The corresponding S_{11} of this geometry is also not able to resonate at any frequency (shown in Figure 3 (Step 3)).

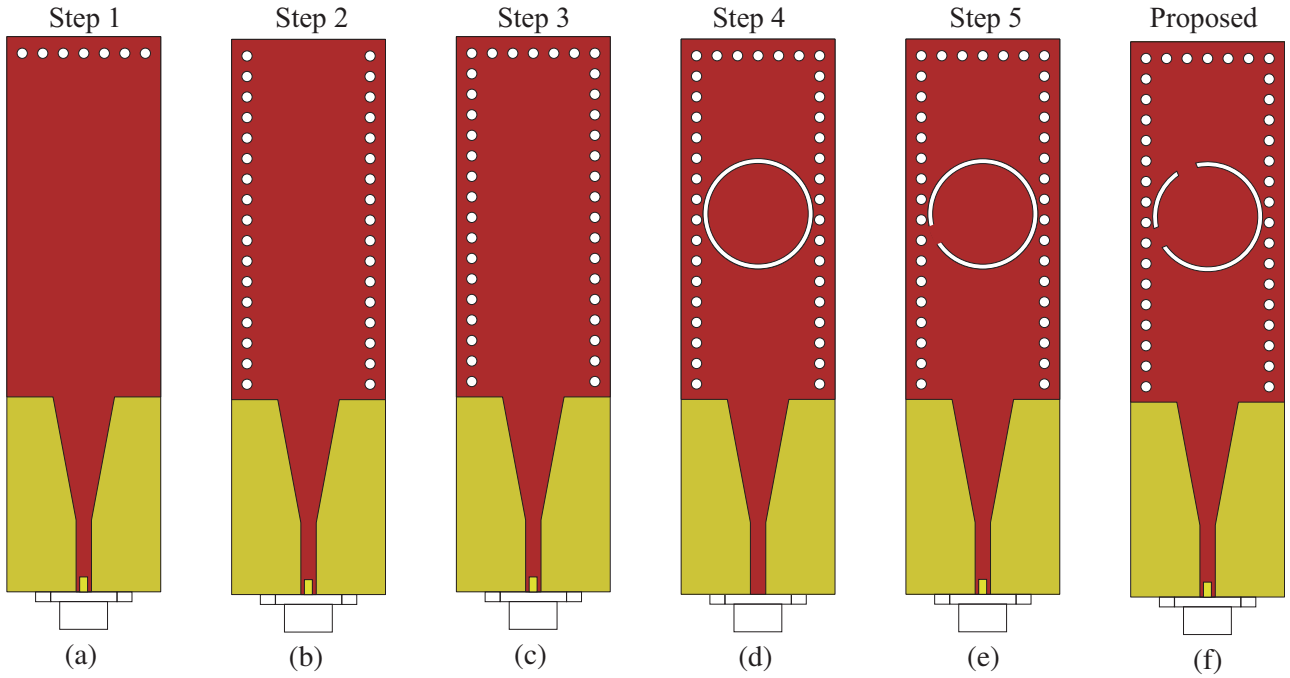

Figure 2. (a)–(f) Proposed geometry evolution steps.

In step 4, a circle is etched on the antenna used in step 3 (shown in Figure 2(d)). The S_{11} of this geometry does not resonate at any frequency (Figure 3 (Step 4)). In step 4, the center ring works as

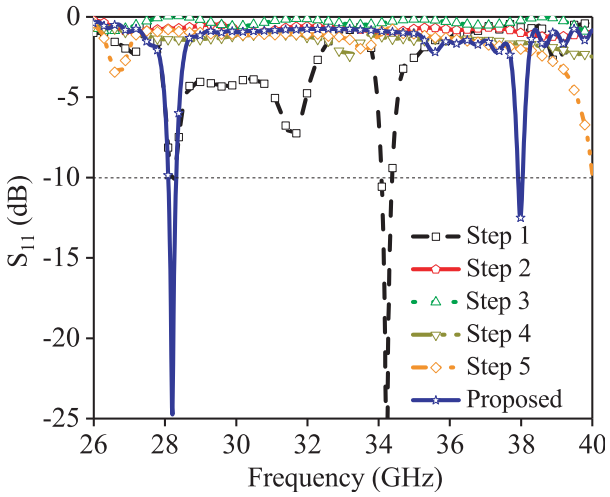

Figure 3. Intermediate step effect on S_{11} magnitude.

a mutually exciting element. In order to connect with the main patch, the cut is introduced in the next step. In step 5, a small cut at θ_1 angle is made in the circle; therefore, the inner part of the circle is connected to the outer part and depicted in Figure 2(e). It is found that the S_{11} using this geometry resonates just outside the required frequency of the designed antenna (depicted in Figure 3 (Step 5)). Finally, in step 6, another cut is made after an angle of $90^\circ + \theta_1$ of the same width as shown in Figure 2(f). This geometry resonates at the required frequencies of the proposed antenna, i.e., at 28 and 38 GHz, which can be seen in Figure 3 (Proposed). Further, it can be noted that the sharp resonance occurs when a circular ring with two cuts is incorporated into the geometry.

2.2. Parametric Analysis

There are many parameters, as shown in Figure 1, that affect the proposed SIW slot antenna. A parametric analysis is carried out with 3D EM simulator CST Microwave Studio to achieve the optimal antenna configuration. Instead of a circular ring, the authors have designed and simulated the SIW antenna with a square ring and triangular ring, and its effect on the reflection coefficient is plotted in

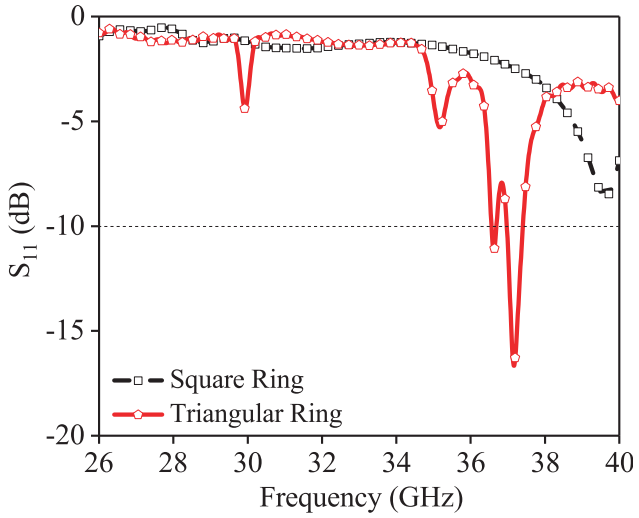

Figure 4. Simulated S_{11} magnitude variation with triangular and square ring.

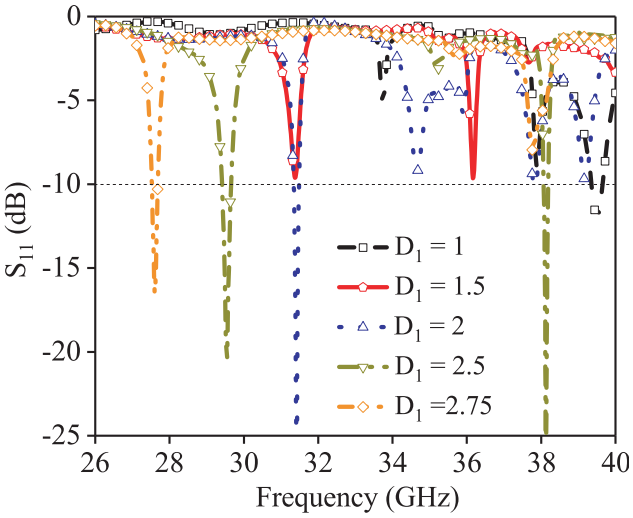

Figure 5. Simulated S_{11} magnitude variation with ring diameter. (Unit: mm).

Figure 4. From Figure 4, it can be seen that for a square ring in the SIW antenna, the antenna cannot resonate in the given frequency range. Further, the triangular ring inside the SIW antenna resonates only at the higher band. For a particular circular ring slot antenna, the designed antenna resonates at 28 and 38 GHz with good bandwidth. The main aim is to design an antenna that should resonate at 28 and 38 GHz, which is satisfied with the help of inserting a circular ring at the center of the patch. Also, the circle has no sharp edges which helps to give good resonance as compared to other geometry.

Further, the introduced circular ring diameters variation and effect on the S_{11} magnitude are given in Figure 5. It can be observed from Figure 5 that the diameter varies from 1 to 2.75 mm. As diameter increases, the resonating frequency is shifted towards the lower side. For particular $D_1 = 2.68$ mm, the antenna resonates in dual-bands. It can be observed that the resonance frequencies are changed as location and dimensions of the ring vary.

3. SIMULATION AND MEASUREMENT RESULTS

In this section, simulation and measurement results of the designed SIW slot antenna are explained. First, the designed SIW slot antenna is fabricated on a Rogers RT-Duroid 5880 substrate with dielectric constant (ϵ_r) of 2.2 and thickness of 0.254 mm. The fabricated prototype of the designed SIW structure is illustrated in Figure 6(a). Also, the top-view and bottom-view of the fabricated prototype are presented. Finally, the design has been simulated using CST-MWS software [17].

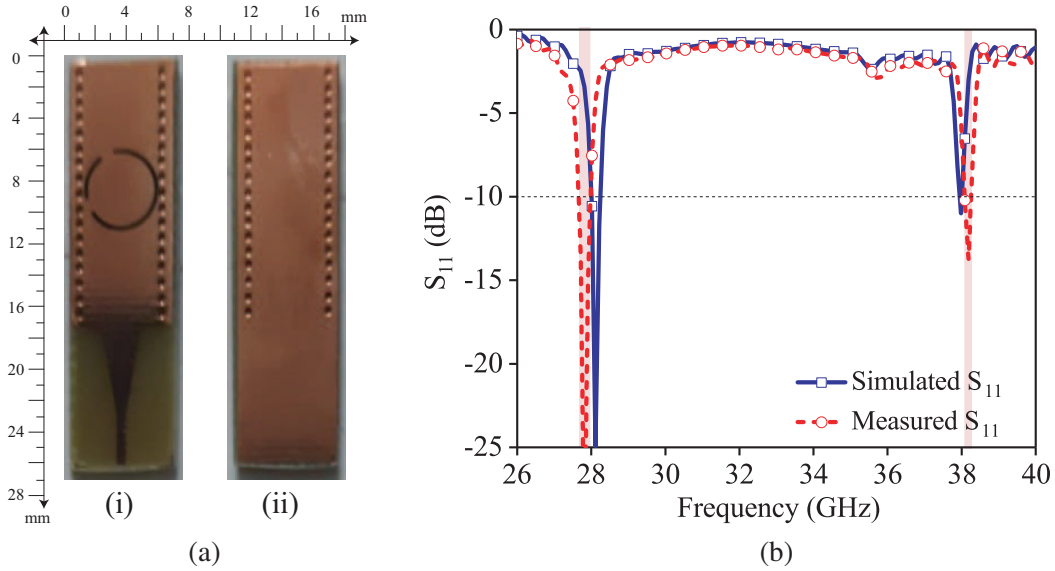

Figure 6. (a) Fabricated prototype. (b) Simulated and measured S_{11} magnitude.

3.1. Reflection Coefficient

A Keysight N5247A PNA-X Microwave Network Analyzer and solder-free V-type (1.85 mm) End-Launch connectors from Southwest Microwave validate the reflection coefficients of the produced prototypes. The simulated and measured S_{11} magnitudes are depicted in Figure 6(b). It can be seen that the antenna resonates at 27.90 and 38.05 GHz with impedance bandwidth of 246.2 and 102.4 MHz, respectively. The prototype completely covers the 28 and 38 GHz bands, making it an excellent contender for 5G dual-band wireless networks. The minor variation in the resonating frequency and reflection coefficient is due to fabrication error and the SMA connector. The achieved simulated and measured reflection coefficient results are acceptable for future 5G applications.

Figure 7(a) and Figure 7(b) show the simulated current flow at fr_1 (i.e., 28 GHz) and fr_2 (i.e., 38 GHz), respectively. It can be seen that the slot edges are responsible for the lower 28 GHz resonance. E-fields are more concentrated at the edge of the slot at 28 GHz. Further, the higher band resonance

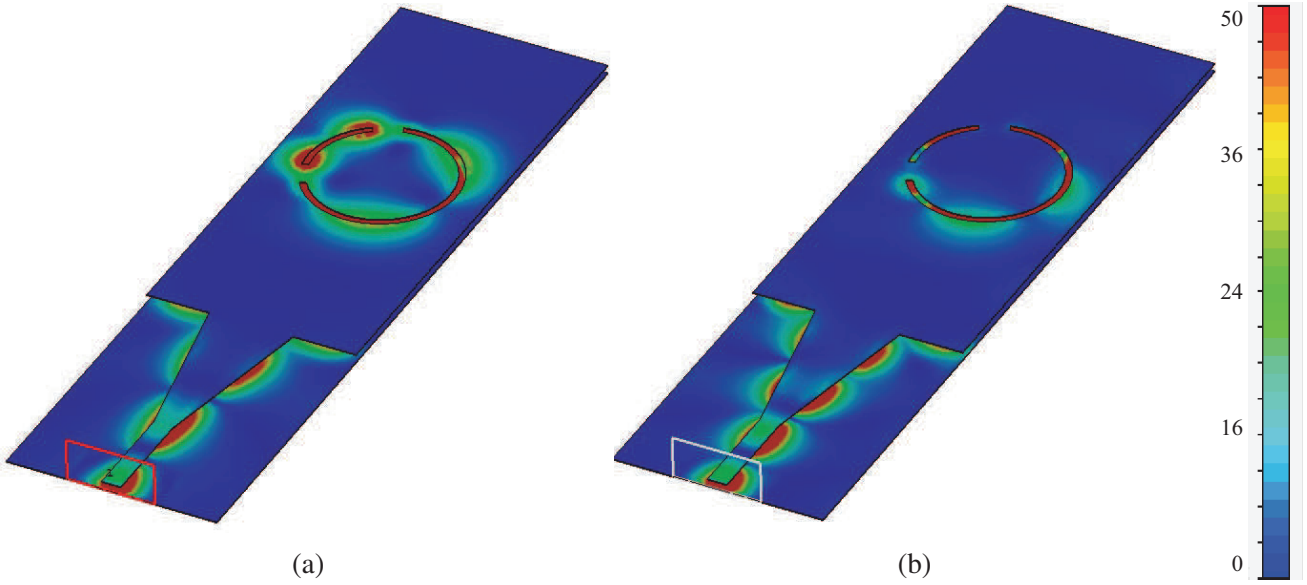

Figure 7. Simulated surface current at: (a) $\mathrm{fr}_1 = 28\,\mathrm{GHz}$, (b) $\mathrm{fr}_2 = 38\,\mathrm{GHz}$.

occurs due to the entire outer ring. From Figure 7(b), the E-fields are more concentrated at the outer ring.

3.2. Radiation Patterns

An NSI-MI spherical near-field measuring range within an anechoic chamber with outside dimensions of $8 \times 4 \times 4\,\mathrm{m}^3$ is used to verify the proposed SIW antenna's far-field performance. In addition, the simulations contain a model of the measuring connection to allow for a proper comparison of observed and simulated radiation patterns.

Figure 8 shows how the proposed SIW slot antenna's observed and computed radiation patterns at 28 GHz correspond well in the E-plane ($\phi = 0°$) and H-plane ($\phi = 90°$). Similarly, the simulated and measured radiation patterns at 38 GHz in both $\phi = 0°$ and $\phi = 90°$ cuts are depicted in Figure 9. It can be noted that the achieved radiation patterns for both resonating bands are directional and acceptable, as well as achieving good suppression of the cross-polarization. Furthermore, the far-field patterns, particularly in the $\phi = 0°$ cut, have a slightly asymmetrical nature. This is due to the large, solid metal measuring connector present in that plane.

Nonetheless, as seen in Figures 8 and 9, there are some modest variations between the produced and observed radiation patterns. More specifically, the main beam in the H-plane has moved somewhat at 28 GHz, and the observed and modelled sidelobe levels at both frequencies do not exactly line up. Even the slightest disturbance in the measuring environment has an influence on the far-field pattern at these high mmWave frequencies.

3.3. Gain and Radiation Efficiency

The simulated and measured gains of the designed SIW slot antenna are illustrated in Figure 10. It can be noted that the measured gain achieved at 27.90 and 38.05 GHz is 7.09 and 8.14 dBi, respectively. The measured directivity at 27.90 and 38.05 GHz is 8.01 and 8.36 dBi, respectively. The simulated radiation efficiency versus frequency is given in Figure 10. It can be noted that the radiation efficiency of the proposed SIW slot antenna is more than 85% over the resonating bands. The simulated and measured performance parameters of the designed SIW antenna are given in Table 2. From Table 2, it can be seen that the simulated and measured results are perfectly matched. The 3D radiation patterns of the proposed SIW slot antenna at the 28 and 38 GHz are given in Figure 11. It can be noted that the directional radiation patterns are achieved, and the main lobe is at $\theta = 0°$ direction.

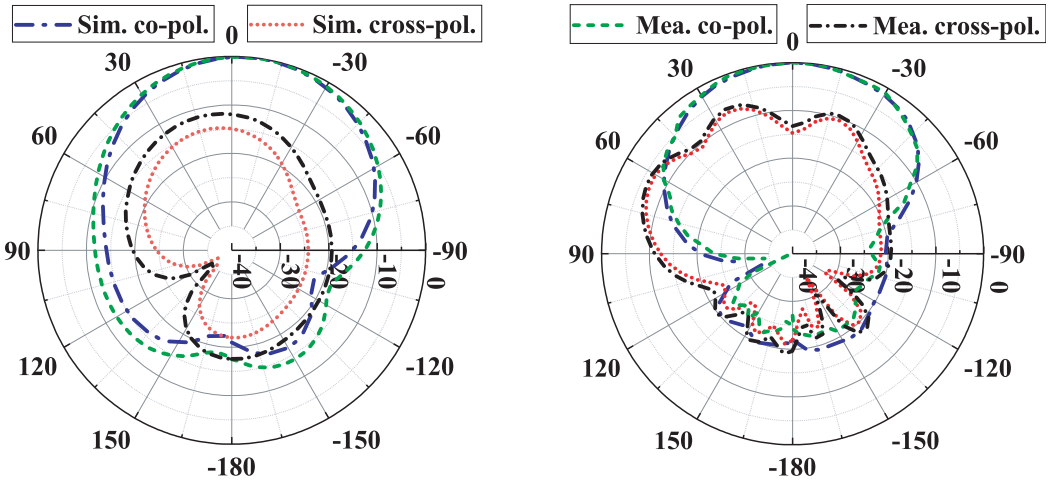

Figure 8. Simulated and measured radiation pattern at $fr_1 = 28$ GHz: (a) Phi = 0°, (b) Phi = 90°.

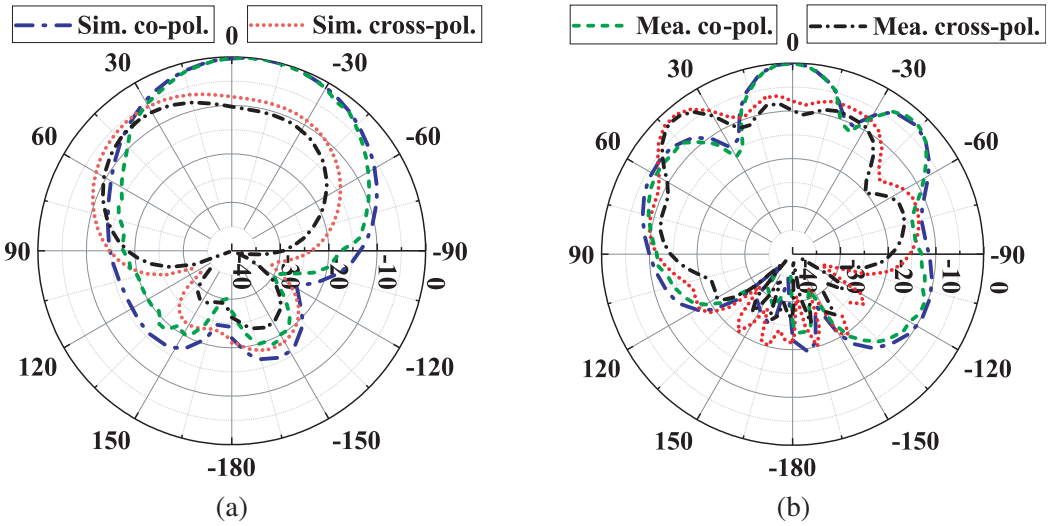

Figure 9. Simulated and measured radiation pattern at $fr_2 = 38$ GHz: (a) Phi = 0°, (b) Phi = 90°.

Table 2. Simulated and measured results.

Parameters	Resonating band 1		Resonating band 2	
	Sim.	Mea.	Sim.	Mea.
Frequency (GHz)	28.13	27.90	37.97	38.05
S_{11} (dB)	−25.33	−27.15	−11.16	−14.20
Bandwidth (MHz)	231.0	246.2	92.0	102.4
Gain (dBi)	7.27	7.09	8.46	8.14
SLL (dB)	−16.0	−15.1	−14.4	−13.1
Directivity (dBi)	8.08	8.01	8.60	8.36
Rad. Efficiency (%)	88.25	–	86.30	–

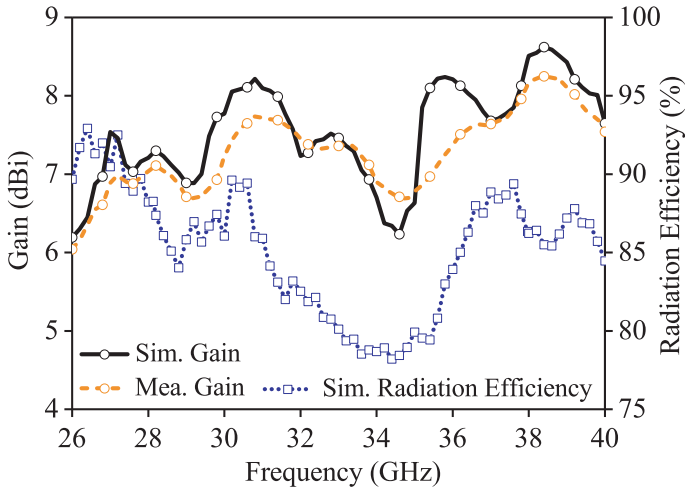

Figure 10. Simulated and measured gain of the proposed geometry as well as simulated radiation efficiency.

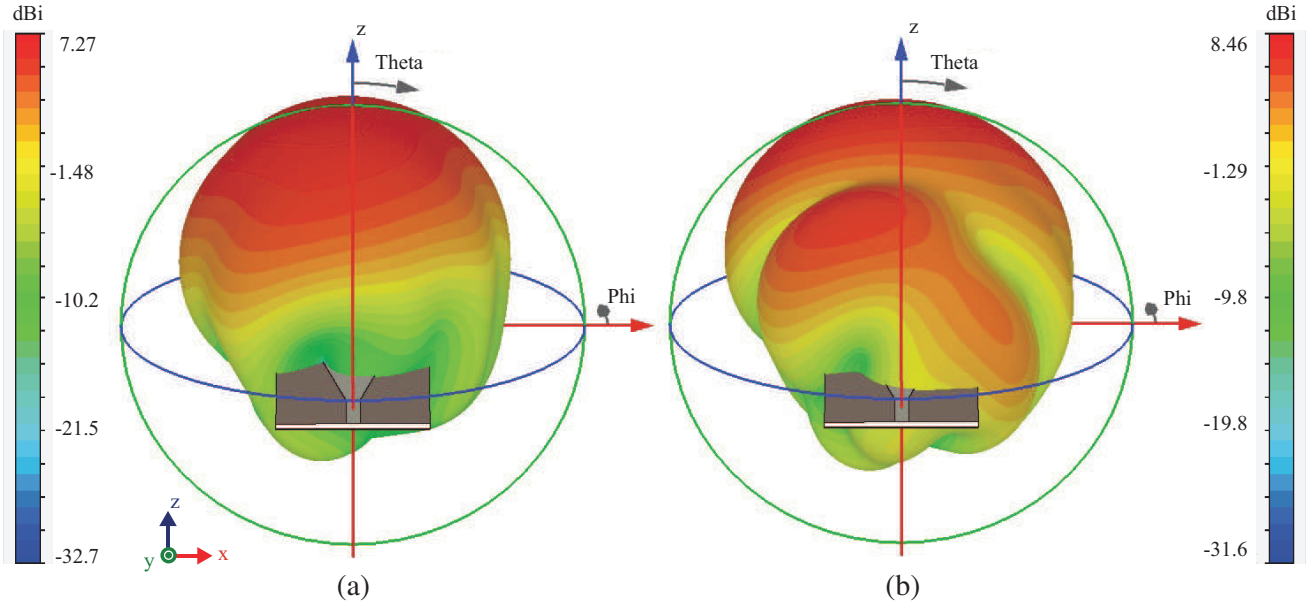

Figure 11. Simulated 3D radiation pattern at $fr_1 = 28\,\text{GHz}$ and $fr_2 = 38\,\text{GHz}$.

Table 3 shows a comparison of the proposed dual-band high gain SIW slot antenna's computed and measured findings, as well as the constructed prototype. From Table 3, it can be seen that the proposed design achieves acceptable resonating bands as well as impedance bandwidth. Also, the designed single layer simple geometry gives good gain and better radiation pattern. Further, the gain of the single element can be improved by incorporating the array topology. Therefore, the proposed SIW slot antenna is a good candidate for future 5G communication applications.

Table 3. Comparison of the proposed SIW slot antenna with other referenced dual-band antennas.

Ref.	No. of Band(s)	Resonating frequency (GHz)	Bandwidth (MHz)	Gain (dBi)	Layer	Permitivity	Thickness (mm)
[7]	Dual	9.5/13.85	190/200	4.8/3.74	Single	2.2	0.787
[8]	Single	46	4720	7.8	Single	2.2	0.25
[9]	Dual	8.28/10.16	390/790	6.1/5.4	Single	2.2	0.787
[10]	Dual	10.3/12.05	510/840	5.23/7.41	Single	2.2	0.787
[11]	Dual	37.5/47.8	400/650	5/5.7	Single	2.2	0.508
[12]	Dual	9.4/15.2	600/700	14.5/17.5	Multi	2.2/3.55	3 and 2
[13]	Dual	28/38	2000/1600	10.1/10.2	Multi	2.2/3.52	0.5 and 0.1
[14]	Dual	28/38	1700/2100	7/3.9	Single	2.2	0.787
[15]	Dual	25.5/40	3900/7600	7.69/10.99	Multi	2.2	–
This work	Dual	27.90/38.05	246.2/102.4	7.09/8.14	Single	2.2	0.25

4. CONCLUSION

The designed dual-band low-profile SIW slot antenna has been applicable to future 5G communication systems. The proposed geometry is excited with 50 Ω microstrip line and resonates at 28 and 38 GHz. The inserted circular slotted ring generates TE_{101} and TE_{102} modes, respectively. The measured impedance bandwidth is 246.2 and 102.4 MHz, and the measured peak gain is 7.09 and 8.14 dBi at 27.90 and 38.05 GHz, respectively. Further, it has more than 85% radiation efficiency over the resonating bands. Also, it gives high directivity and better radiation patterns with low sidelobe levels. The suggested SIW slotted antenna is a good contender for future 5G dual-band communication systems based on these findings.

REFERENCES

1. Sulyman, A. I., A. T. Nassar, M. K. Samimi, G. R. MacCartney, T. S. Rappaport, and A. Alsanie, "Radio propagation path loss models for 5G cellular networks in the 28 GHz and 38 GHz millimeter-wave bands," *IEEE Communications Magazine*, Vol. 52, No. 9, 78–86, 2014.
2. Stevenson, A. F., "Theory of slots in rectangular wave-guides," *J. Appl. Phys.*, Vol. 19, 24–38, 1948.
3. Bozzi, M., A. Georgiadis, and K. Wu, "Review of substrate-integrated waveguide circuits and antennas," *IET Microwaves, Antennas & Propagation*, Vol. 5, No. 8, 909–920, 2011.
4. Liu, J., X. Tang, Y. Li, and Y. Long, "Substrate integrated waveguide leaky-wave antenna with H-shaped slots," *IEEE Transactions on Antennas and Propagation*, Vol. 60, No. 8, 3962–3967, 2012.
5. Balanis, C. A., *Antenna Theory: Analysis and Design*, Wiley, Hoboken, NJ, USA, 2016.
6. Patanvariya, D. G. and A. Chatterjee, "Modified-T shaped wideband antenna for Ka-band applications," *International Conference on Communication and Signal Processing (ICCSP)*, 1654–1658, 2020.
7. Mukherjee, S., A. Biswas, and K. V. Srivastava, "Substrate integrated waveguide cavity-backed dumbbell-shaped slot antenna for dual-frequency applications," *IEEE Antennas and Wireless Propagation Letters*, Vol. 14, 1314–1317, 2014.

8. Xie, H., L. Belostotski, and M. Okoniewski, "A Q-band high-gain substrate-integrated waveguide slot antenna," *Microwave and Optical Technology Letters*, Vol. 57, No. 6, 1370–1374, 2015.
9. Mukherjee, S. and A. Biswas, "Design of dual band and dual-polarised dual band SIW cavity backed bow-tie slot antennas," *IET Microwaves, Antennas & Propagation*, Vol. 10, No. 9, 1002–1009, 2016.
10. Nandi, S. and A. Mohan, "Bowtie slotted dual-band SIW antenna," *Microwave and Optical Technology Letters*, Vol. 58, No. 10, 2303–2308, 2016.
11. Wu, Q., J. Yin, C. Yu, H. Wang, and W. Hong, "Low-profile millimeter-wave SIW cavity-backed dual-band circularly polarized antenna," *IEEE Transactions on Antennas and Propagation*, Vol. 65, No. 12, 7310–7315, 2017.
12. Wei, D. J., J. Li, G. Yang, J. Liu, and J. J. Yang, "Design of compact dual-band SIW slotted array antenna," *IEEE Antennas and Wireless Propagation Letters*, Vol. 17, No. 6, 1085–1089, 2018.
13. Deckmyn, T., M. Cauwe, D. V. Ginste, H. Rogier, and S. Agneessens, "Dual-band (28, 38) GHz coupled quarter-mode substrate-integrated waveguide antenna array for next-generation wireless systems," *IEEE Transactions on Antennas and Propagation*, Vol. 67, No. 4, 2405–2412, 2019.
14. Lai, F. P., L. W. Chang, and Y. S. Chen, "Miniature dual-band substrate integrated waveguide slotted antenna array for millimeter-wave 5G applications," *International Journal of Antennas and Propagation*, Vol. 3, 1–10, 2020.
15. Feng, B., X. He, and J. C. Cheng, "Dual-wideband dual-polarized metasurface antenna array for the 5G millimeter wave communications based on characteristic mode theory," *IEEE Access*, Vol. 8, 21589–21601, 2020.
16. Patanvariya, D. G. and A. Chatterjee, "A compact bow-tie shaped wide-band microstrip patch antenna for future 5G communication networks," *Radioengineering*, Vol. 30, No. 1, 2021.
17. CST Studio Suite, Computer Simulation Technology, [Online], Available: https://www.cst.com.